

tically from  $-80 \pm 40$  K for  $T > T_N$  to  $-10 \pm 5$  K for  $T < T_N$ . With changing impurity concentration in the same alloy (at  $T < T_N$ ) the value of  $\Theta$  can change from  $-60 \pm 10$  K at  $n_{Fe} \sim 0.5\%$  to  $+6 \pm 2$  K at  $n_{Fe} \sim 3.5\%$ .<sup>15</sup>

- <sup>1</sup>L. V. Keldysh and Yu. V. Kopaev, *Fiz. Tverd. Tela (Leningrad)* **6**, 2791 (1964) [*Sov. Phys. Solid State* **6**, 2219 (1964)].  
<sup>2</sup>B. I. Halperin and T. M. Rice, *Solid State Phys.* **21**, 115 (1968).  
<sup>3</sup>P. A. Fedders and P. C. Martin, *Phys. Rev.* **143**, 245 (1966).  
<sup>4</sup>T. M. Rice, *Phys. Rev. B* **2**, 3619 (1970).  
<sup>5</sup>J. Kondo, *Prog. Theor. Phys.* **32**, 37 (1964).  
<sup>6</sup>B. A. Volkov, Yu. V. Kopaev, and A. I. Rusinov, *Zh. Eksp. Teor. Fiz.* **68**, 1899 (1975) [*Sov. Phys. JETP* **41**, 952 (1975)].  
<sup>7</sup>Yu. V. Kopaev and A. I. Rusinov, *Fiz. Tverd. Tela (Leningrad)* **11**, 1306 (1969) [*Sov. Phys. Solid State* **11**, 1059 (1969)].  
<sup>8</sup>P. W. Anderson, *Phys. Rev.* **124**, 41 (1961).  
<sup>9</sup>A. Angel, M. Barlea, and M. Crisan, *Solid State Commun.* **28**, 711 (1978).  
<sup>10</sup>E. Wachtel and V. Vetter, *Z. Metallkd.* **52**, 525 (1961).

- <sup>11</sup>W. Koster, E. Wachtel, and K. Crube, *Z. Metallkd.* **54**, 393 (1963).  
<sup>12</sup>A. Kallel and De Bergevin, *Solid State Commun.* **5**, 955 (1967).  
<sup>13</sup>S. Arajs, L. N. Reeves, and E. E. Anderson, *J. Appl. Phys.* **42**, 1691 (1971).  
<sup>14</sup>K. Fukamichi and H. Saito, *J. Phys. Soc. Jpn.* **33**, 1485 (1972).  
<sup>15</sup>V. A. Makarov, B. N. Tret'yakov, N. M. Puzei, G. P. Kalinin, and V. A. Tokmakova, *Fiz. Tverd. Tela (Leningrad)* **21**, 901 (1979) [*Sov. Phys. Solid State* **21**, 527 (1979)].  
<sup>16</sup>T. Suzuki, *J. Phys. Soc. Jpn.* **21**, 442 (1966).  
<sup>17</sup>F. Hedgcock, J. Strom-Olsen, and D. Wilford, *J. Phys. F: Metal. Phys.* **7**, 855 (1977).  
<sup>18</sup>Y. Ishikawa, S. Hoshio, and Y. Endoh, *J. Phys. Soc. Jpn.* **22**, 1221 (1967).  
<sup>19</sup>Y. Hamaguchi and N. Kunitomi, *J. Phys. Soc. Jpn.* **19**, 1849 (1964).  
<sup>20</sup>Y. Nakai, *J. Phys. Soc. Jpn.* **33**, 1348 (1972).  
<sup>21</sup>I. Pop, V. Iusan, and A. Giurgiu, *Phys. Lett.* **49A**, 439 (1974).  
<sup>22</sup>R. A. Ruderman and Ch. Kittel, *Phys. Rev.* **96**, 99 (1954).

Translated by J. G. Adashko

## Ferrimagnets with Ising ions. Magnetic properties of holmium-yttrium iron garnets in strong fields at helium temperatures

V. I. Silant'ev, A. I. Popov, R. Z. Levitin, and A. K. Zvezdin

*Moscow State University*

(Submitted 5 July 1979)

*Zh. Eksp. Teor. Fiz.* **78**, 640-655 (February 1980)

The magnetization of single-crystal holmium-yttrium iron garnets  $\text{Ho}_x\text{Y}_{3-x}\text{Fe}_5\text{O}_{12}$  ( $0 \leq x \leq 3$ ) was measured in fields up to 300 kOe at 4.2 K. It was observed that phase transitions into field-induced noncollinear phases in compositions with  $x < 1.65$  are of first order  $H$ - $x$  phase diagrams of holmium-yttrium iron garnets are constructed for field orientations along the crystallographic axes  $\langle 111 \rangle$ ,  $\langle 110 \rangle$ , and  $\langle 100 \rangle$ . It is shown that the experimental data (the magnetization curves along different directions, the dependences of the transition fields on the holmium concentration and on the orientation of the magnetic field, etc.) of ferrites with  $x < 1.65$  can be explained by means of a model that considers the  $\text{Ho}^{3+}$  ion in the garnet structure in an extremely anisotropic Ising approximation. Possible causes of deviation from this model in iron garnets with large holmium contents are discussed.

PACS numbers: 75.30.Cr, 75.30.Kz, 75.50.Gg

### 1. INTRODUCTION

Numerous recent investigations (see, e.g., the review<sup>1</sup>) have shown that noncollinear magnetic structures can be produced in ferrimagnets in a certain field interval. The formation of such structures is due to the competition between the negative exchange interaction that tends to produce an antiparallel alignment of the magnetic moments of the sublattices of the ferrimagnet, and the Zeeman interaction of the magnetic moment of the sublattices with the external field, which tends to orient them parallel to each other.

The field-induced noncollinear magnetic structures were investigated in greatest detail theoretically and

experimentally in ferrimagnets in which the magnetic anisotropy is either nonexistent (the isotropic case)<sup>2</sup> or is small compared with the exchange interaction between the sublattices.<sup>3</sup> Much less investigated were the noncollinear structures in strongly anisotropic ferrimagnets. Anomalies of the magnetization of holmium-yttrium iron garnets (HYIG)  $\text{HO}_x\text{Y}_{3-x}\text{Fe}_5\text{O}_{12}$  ( $x \leq 0.4$ ) were observed in Ref. 4 in fields close to the exchange field ( $\sim 10^5$  Oe). It was shown theoretically<sup>5</sup> that these anomalies can be interpreted as a manifestation of the realignment of the magnetic structure of the ferrimagnet in the field. The rare-earth holmium ions were treated in this case in the extremely anisotropic Ising approximation.

However, the earlier experimental data<sup>4</sup> and the corresponding theoretical calculations<sup>5</sup> pertained to HYIG with small holmium content and the question of whether the proposed model describes the HYIG with large numbers of holmium ions remained open. In addition, principal attention was paid in Refs. 4 and 5 to the magnetization anomalies in strong fields comparable with the exchange fields, and practically no analysis (theoretical or experimental) was made of the magnetization curves of Ising ferrimagnets in weaker fields. We have therefore undertaken experimental investigations of the magnetic properties of single crystals of the HYIG system  $\text{Ho}_x\text{Y}_{3-x}\text{Fe}_5\text{O}_{12}$  in a wide range of concentrations ( $0 \leq x \leq 3$ ) and of magnetic fields (up to 300 kOe) at liquid-helium temperature, and calculated the magnetization and the phase diagram of these ferrimagnets in a model that takes into account the Ising character of the holmium ions  $\text{Ho}^{3+}$ . The experimental results were compared with this theoretical model. The possible causes that lead in a number of cases to a difference between the experimental and theoretical data were analyzed.

## 2. FUNDAMENTAL MAGNETIC PROPERTIES OF RARE-EARTH IRON GARNETS

The rare-earth iron garnets (REIG)  $\text{R}_3\text{Fe}_5\text{O}_{12}$  ( $R$  is a rare-earth element or yttrium) had a cubic crystal structure and are described by the space group  $O_h^{10}$ . The  $\text{Fe}^{3+}$  ions in the garnet crystal lattice (the unit cell contains eight formula units  $\text{R}_3\text{Fe}_5\text{O}_{12}$ ) occupy places with octahedral oxygen surrounding ( $a$ -sites) and places with tetrahedral oxygen surrounding ( $d$ -sites). A strong negative exchange interaction takes place between the  $\text{Fe}^{3+}$  ions in the  $a$  and  $d$  sites (the effective field is  $H_{a-d} \approx 2 \cdot 10^6$  Oe) and leads to antiparallel orientation of the magnetic moments of the  $\text{Fe}^{3+}$  ions in these places, so that in the fields  $H \ll H_{a-d}$  we can consider one  $a$ - $d$  sublattice of the iron ions with a magnetic moment  $M_{\text{Fe}}$  equal to the difference between the magnetic moments of the  $a$  and  $d$  sublattices (at 0 K we have  $M_{\text{Fe}} = 5\mu_B$  per formula unit).

The rare-earth ions  $\text{R}^{3+}$  are located in sites with dodecahedral surroundings of oxygen ions, having a point group  $D_2$  ( $c$ -sites), while the crystal lattice has six non-equivalent  $c$ -sites that differ in the orientation of the axes of the dodecahedron (Fig. 1). In the general case it is therefore necessary to consider six different rare-earth sublattices. The magnetic ordering of the rare-earth ions is due to the negative exchange interaction with the iron sublattice. The effective field of the R-Fe interaction is of the order of  $10^5$  Oe, i.e., it is weaker than the Fe-Fe interaction. The exchange interaction between the rare-earth ions is weak, and can be neglected. Thus, in mixed REIG  $\text{R}_x\text{Y}_{3-x}\text{Fe}_5\text{O}_{12}$  the exchange field acting on the rare-earth ion can be regarded in first-order approximation as independent of the concentration of the rare-earth ions.

## 3. THEORY

We examine the properties of mixed REIG  $\text{R}_x\text{Y}_{3-x}\text{Fe}_5\text{O}_{12}$  as functions of the field and of the con-

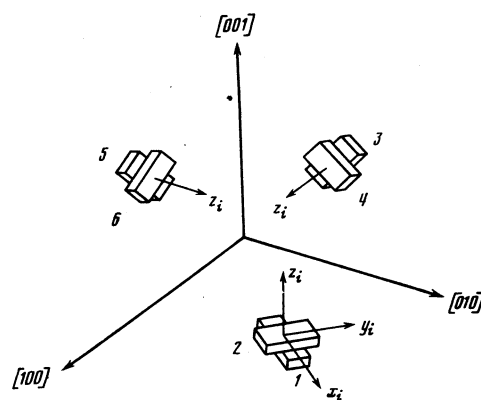


FIG. 1. Arrangement of the six nonequivalent dodecahedra in the unit cell of the garnet.

centration of the rare-earth ions at 0° K. Just as previously,<sup>5</sup> we describe the  $\text{R}^{3+}$  ions in the Ising approximation, i.e., we assume that at all orientations of the fields (external magnetic field and exchange field) acting on this ion the magnetic moment of the ion can be oriented only along a definite Ising axis that coincides with some particular symmetry axis of that  $c$ -site at which the rare-earth ion is located. As the Ising axis of each  $i$ -th site we chose<sup>5</sup> the  $z_i$  axis (see Fig. 1). Since this choice is the only one at which the resultant easy-magnetization axes of the garnet coincide with axes of the type  $\langle 111 \rangle$ , as is the case for most REIG and in particular for the HYIG considered below. We note that with this choice of axes the positions 1 and 2, 3 and 4, and 5 and 6 become pairwise equivalent and we consider three magnetic sublattices of the rare-earth ions.

Although the proposed model is hypothetical and its correctness is confirmed only by the agreement between the theoretical predictions and the experimental data, it is based in many respects on results of investigations of the state of rare-earth ions in the garnet structure. The crystal fields produced at the rare-earth ion by the surrounding oxygen split the principal multiplet of this ion into doublets for Kramers ions and singlets for non-Kramers ions. In a number of cases the lower levels in the spectrum of non-Kramers ions are two closely-lying singlets located far enough from the higher levels (see, e.g. Ref. 6). As shown by Griffith,<sup>7</sup> these ions behave like Ising ions.

We proceed now to construct the thermodynamic potential (the energy of the ground state of the system). The effective field acting on the rare-earth ion can be represented in the usual form

$$H_{\text{eff}} = H - \lambda M_{\text{Fe}}, \quad (1)$$

where  $H$  is the external field,  $M_{\text{Fe}}$  is the magnetic moment of the iron sublattice, and  $\lambda > 0$  is the constant of the molecular field produced at the rare-earth ion by the iron sublattice.

Since we assume an Ising rare-earth ion, the levels of the quasidoublet of the ion in the  $i$ -th site will be split only by the  $z_i$  component of the effective field, and the energy of the ground state of such a ferrimagnet (per molecule of the REIG) can be written in the form

(see Ref. 5)

$$E = -\frac{x\mu_R}{3} \sum_{i=1,3,5} |(\mathbf{H} - \lambda \mathbf{M}_{Fe}) \mathbf{z}_i| - \mathbf{M}_{Fe} \mathbf{H}, \quad (2)$$

where  $\mu_R$  is the magnetic moment of the rare-earth ion,  $x$  is the concentration, and  $\mathbf{z}_i$  is a unit vector. (Formula (2) can be represented in the form

$$E = -\frac{1}{3} x \mu_R [ |H_{eff}^x| + |H_{eff}^y| + |H_{eff}^z| ] - \mathbf{M}_{Fe} \mathbf{H}, \quad (3)$$

where  $H_{eff}^x, H_{eff}^y, H_{eff}^z$  are the projections, on the coordinate axes of the effective field acting on the rare-earth sublattice. The first term in this expression describes the magnetic anisotropy and, as seen from (3) in this model the magnetic anisotropy does not reduce to the form usual for cubic weakly anisotropic ferrimagnets.)

Denoting by  $\mathbf{l}_i$  the direction of the magnetic moment of the rare-earth ion in the  $i$ -th position

$$\mathbf{l}_i = \mathbf{z}_i \text{sign} \{ (-\lambda \mathbf{M}_{Fe} + \mathbf{H}) \mathbf{z}_i \}, \quad (4)$$

we represent the energy of the ground state in the form

$$E = -\mathbf{M}_{Fe} \mathbf{H} - \frac{x\mu_R}{3} \sum_{i=1,3,5} (\mathbf{H} - \lambda \mathbf{M}_{Fe}) \mathbf{l}_i. \quad (5)$$

Changing over to the dimensionless variables

$$\varepsilon = E/M_{Fe}(\lambda M_{Fe}), \quad h = H/\lambda M_{Fe},$$

we obtain

$$\varepsilon = -\gamma(h - m_R) - hm_R, \quad (6)$$

where  $\gamma = \mathbf{M}_{Fe} / M_{Fe}$ , and the vector

$$\mathbf{m}_R = \frac{x\mu_R}{3M_{Fe}} \sum_{i=1,3,5} \mathbf{l}_i \quad (7)$$

is the combined moment of the rare-earth ions in relative units. Its value

$$m_R = x\mu_R/3^0 M_{Fe} \quad (8)$$

can be regarded as the relative concentration of the rare-earth ions, so that we shall investigate henceforth the behavior of an equilibrium configuration of magnetic moment of the system as a function of the field at different values of  $m_R$  (i.e., of  $x$ ).<sup>1)</sup>

Since the magnetic moment of the rare-earth ion in each  $i$ -th site is oriented collinear with the corresponding  $\mathbf{z}_i$  axis, i.e., collinear with a crystallographic axis of the type  $\langle 100 \rangle$ , it follows that the summary magnetic moment of all the rare-earth ions,  $\mathbf{m}_R$ , can be directed at 0°K only along an axis of the type  $\langle 111 \rangle$ . Thus, magnetic phase transitions can proceed in this system, depending on the field, only via discrete reorientations of the magnetic moment  $\mathbf{m}_R$  of the summary rare-earth sublattice from  $\mathbf{m}_R$  from one direction of the type  $\langle 111 \rangle$  to another (with a corresponding rotation of the magnetic moment of the iron sublattice). The phases of the system are determined by the direction of the vector  $\mathbf{m}_R$ , and, as is clear from the foregoing, the maximum possible number of phases is eight. Naturally, not all eight phases are realized each time. The ratio of the magnetic moments of the rare-earth and iron sublattices specifies the initial phase  $H \rightarrow 0$ , and when the field is increased only the phases corresponding to the energy minimum are realized.

The equilibrium direction of the magnetization of the iron sublattice at a given  $m_R$  is determined by minimization of (6) with respect to  $\gamma$  given by

$$\gamma = (h - m_R) / |h - m_R|. \quad (9)$$

Thus, in the phase specified by the orientation of the vector  $\mathbf{m}_R$ , the equilibrium magnetic moment of the system (normalized to  $M_{Fe}$ ) is

$$\mathbf{m} = \gamma + \mathbf{m}_R = \mathbf{m}_R + (h - m_R) / |h - m_R|, \quad (10)$$

and its projection on the direction of the field (its magnetization) is

$$m_{||} = \frac{(m_R h)}{h} - \frac{h - m_R h / h}{|h - m_R|}. \quad (11)$$

Substituting (9) in (6), we find that the energy of the ground state in a phase with specified  $m_R$  is

$$\varepsilon = -|h - m_R| - hm_R. \quad (12)$$

The regions of existence of phases on the  $(h, m_R)$  plane can be easily obtained from the condition that the given phase, determined by the direction of  $\mathbf{m}_R$ , ceases to exist when the projection of the effective field

$$h_{eff} = h - (h - m_R) / |h - m_R| \quad (13)$$

on any of the axes  $\mathbf{z}_i$  (or, equivalently, on the crystallographic axes  $[100], [010], [001]$ ) vanishes. In fact, as follows from (4), the reversal of the sign of the projection of the effective field on the  $\mathbf{z}_i$  axis causes a reorientation of the magnetic moment of the rare-earth ion in the  $i$ -th site, and this leads to a change in the orientation of the vector  $\mathbf{m}_R$  [see (7)].

Thus, the problem of finding the equilibrium configurations of the magnetic moments of a given system and of the phase transitions between them reduces to the following: a) determination of the regions of existence of phases with specified  $m_R$ ; b) calculation of the energy of these phases by formula (12) and determination of the phase with the lowest energy for given  $H$  and  $x$ ; c) finding the phase-transition lines from the condition that the phase energies be equal.

We consider first the phase diagrams of Ising ferrimagnets at 0°K for the three field orientations most frequently encountered in experiment:  $h \parallel [001]$ ,  $h \parallel [110]$  and  $h \parallel [111]$ .

A.  $h \parallel [001]$ . At this orientation of the field, two fourfold degenerate phases are possible:

- 1)  $m_R \parallel [\bar{1}\bar{1}\bar{1}]$ ,  $m_R \parallel [1\bar{1}\bar{1}]$ ,  $m_R \parallel [\bar{1}1\bar{1}]$ ,  $m_R \parallel [11\bar{1}]$ ;
- 2)  $m_R \parallel [\bar{1}11]$ ,  $m_R \parallel [111]$ ,  $m_R \parallel [\bar{1}\bar{1}1]$ ,  $m_R \parallel [1\bar{1}1]$ .

and have different projections of the vector  $\mathbf{m}_R$  on the field direction. The first-order phase-transition line that separates these phases is determined from equality of their energies and is of the form<sup>2)</sup>

$$h_{1 \rightarrow 2} = 3^0 [(m_R^2 - 1) / (m_R^2 - 3)]^0. \quad (14)$$

B.  $h \parallel [110]$ . In this case three phases exist: 1) the doubly degenerate phase  $m_R \parallel [\bar{1}\bar{1}\bar{1}]$ ,  $m_R \parallel [111]$ ; 2) the fourfold degenerate phase  $m_R \parallel [\bar{1}11]$ ,  $m_R \parallel [1\bar{1}1]$ ,  $m_R \parallel [111]$ ,  $m_R \parallel [\bar{1}\bar{1}\bar{1}]$ ; 3) the doubly degenerate phase  $m_R \parallel [111]$ ,  $m_R \parallel [1\bar{1}\bar{1}]$ . The first-order phase-transition line between phases 1) and 2) is given by

$$h_{1 \rightarrow 2} = -\frac{6^{1/2} m_R}{6 - m_R^2} + \left[ \frac{6 m_R^2}{(6 - m_R^2)^2} - \frac{6(m_R^2 - 1)}{6 - m_R^2} \right]^{1/2}, \quad (15)$$

and the first-order transition line between phases 2 and 3 is described by the expression

$$h_{2 \rightarrow 3} = \frac{6^{1/2} m_R}{6 - m_R^2} \pm \left[ \frac{6 m_R^2}{(6 - m_R^2)^2} - \frac{6(m_R^2 - 1)}{6 - m_R^2} \right]^{1/2}. \quad (16)$$

C.  $h \parallel [111]$ . At this field orientation there are four phases: 1) nondegenerate phase  $m_R \parallel [\bar{1}\bar{1}\bar{1}]$ ; 2) three-fold degenerate phase  $m_R \parallel [\bar{1}\bar{1}1]$ ,  $m_R \parallel [\bar{1}1\bar{1}]$ ,  $m_R \parallel [1\bar{1}\bar{1}]$ ; 3) threefold degenerate phase  $m_R \parallel [11\bar{1}]$ ,  $m_R \parallel [111]$ ,  $m_R \parallel [\bar{1}11]$ ; 4) nondegenerate phase  $m_R \parallel [111]$ .

The phase-transition lines between the phases are given by

$$h_{1 \rightarrow 2} = 3(1 - m_R)/(3 - m_R), \quad (17)$$

$$h_{2 \rightarrow 3} = 3[(m_R^2 - 1)/(m_R^2 - 9)]^{1/2}, \quad (18)$$

$$h_{3 \rightarrow 4} = 3(m_R \pm 1)(3 \mp m_R)/(9 - m_R^2), \quad m_R \leq 3^{1/2}. \quad (19)$$

We note that in the region of the existence of phase 4) there exists also one phase transition  $4' - 4''$ , which follows the line

$$h_{4' \rightarrow 4''} = m_R, \quad m_R \geq 3^{1/2}. \quad (20)$$

In this transition, a reorientation of the magnetic moment of the iron sublattices takes place from  $\gamma \parallel -h$  to  $\gamma \parallel h$ , i.e., a transition from a ferrimagnetic structure of the rare-earth and iron sublattices to a ferrimagnetic structure. Within the framework of the considered model, this is a hysteresis-free first-order transition. Hysteresis appears when account is taken of the magnetic anisotropy of the iron sublattice.

We note also that phases 1) and 4) differ from the other phases presented above: their total moment and the moment of the rare-earth sublattice, are collinear with the direction of the field (they can therefore be called collinear or symmetric), whereas in all other phases the total magnetic moment makes an angle with the field direction, the magnitude of this angle being dependent on the value of the field (these phases can be called canted).

We have considered the realignment of the magnetic structure of an Ising ferrimagnet for the most symmetrical directions of the magnetic field. It is important that in these cases, owing to the high symmetry of the system, phase degeneracy took place. The maximum number of phase transitions is equal to 1, 2, or 3 respectively at  $h \parallel \langle 100 \rangle$ ,  $h \parallel \langle \bar{1}00 \rangle$ ,  $h \parallel \langle 111 \rangle$ . Obviously, at other (low-symmetry) directions of the external field the degree of phase degeneracy decreases, and therefore the number of phase transitions increases.

We shall examine this question in greater detail for the case of an arbitrary orientation of the field in the  $(1\bar{1}0)$  plane. In this case there exist the following energywise nonequivalent phases: 1)  $m_R \parallel [\bar{1}\bar{1}\bar{1}]$ , 2)  $m_R \parallel [\bar{1}\bar{1}1]$ ,  $m_R \parallel [1\bar{1}\bar{1}]$ , 3)  $m_R \parallel [11\bar{1}]$ , 4)  $m_R \parallel [111]$ , 5)  $m_R \parallel [\bar{1}11]$ ,  $m_R \parallel [1\bar{1}1]$ , 6)  $m_R \parallel [111]$ . The maximum number of phase transitions is five. The phase-transition lines between the phases are determined by the expression

$$h_{i \rightarrow j} = \frac{2m_R(q_i + q_j)}{4 - m_R^2(q_i - q_j)^2} \pm 2 \left\{ \frac{1 - m_R^2}{4 - m_R^2(q_i - q_j)^2} + \frac{m_R^2(q_i + q_j)^2}{[4 - m_R^2(q_i - q_j)^2]^2} \right\}^{1/2}, \quad (21)$$

where  $q_k = (m_{Rk} \cdot h)/m_R h$  is the projection of the magnetic moment of the rare-earth ions in the  $k$ -th phase on the field direction. A calculation of the dependence of the fields of the phase transitions on the angle of orientation of the field in the  $\{110\}$  plane and a comparison of the experimental and theoretical data will be presented below.

Since the total number of phases, as indicated above, is eight, the maximum possible number of transitions at an arbitrary direction of the magnetic field in space, when the phase degeneracy is completely lifted, is equal to seven. It should be noted, however, that there exists an infinite number of field directions which are not connected with any of the crystal symmetry elements, but for which degeneracy of the phase exists nevertheless. This situation takes place at field orientations  $h \parallel [i, j, k]$ , when the sum (or difference) of any two of the indices  $i$ ,  $j$ , and  $k$  is equal in absolute value to the third. In this case there are at least two energywise equivalent directions  $m_R$ , the projections of which on the field directions are identical (equal to zero), and form by virtue of this a single degenerate phase. Thus, for example, at  $h \parallel [i, j, i + j]$  the phases with orientations  $m_R \parallel [11\bar{1}]$  and  $m_R \parallel [1\bar{1}\bar{1}]$  are energywise equivalent. Therefore the problem of the experimental resolution of all seven discontinuities entails a certain difficulty: an arbitrary direction of the field turns out to be sufficiently close either to the symmetry axes and planes, or to the directions described above.

We have considered the magnetic phase diagrams of iron garnets with Ising rare-earth ions. The magnetization in each phase can be easily obtained from the general formula (11). The theoretical  $m_i(h)$  dependences will be analyzed in greater detail below when the comparison with the experimental data is made. We note here that in Ising ferrimagnets the transitions between the phases are always of first order, therefore the phase-transition fields should always reveal magnetization jumps due to the reorientation of the magnetic moment of the rare-earth sublattice from one of the axes of the  $\langle 111 \rangle$  type to another, with a corresponding rotation of the magnetic moment of the iron sublattice. This constitutes one of the substantial differences between Ising ferrimagnets and ferrimagnets that have a magnetic anisotropy that is small compared with the exchange interaction; in the latter the transitions to the noncollinear phase can be of either first or second order.<sup>3</sup>

Another singularity of Ising ferrimagnets, which we must point out, is that at all field directions except parallel to the easy magnetization axes  $\langle 111 \rangle$ , a noncollinear structure appears already at  $h \rightarrow 0$  and exists in the given approximation up to  $h \rightarrow \infty$ . In weakly anisotropic ferrimagnets, the noncollinear phase exists in most cases in a limited field interval.<sup>3</sup>

#### 4. SAMPLES AND MEASUREMENT PROCEDURES

Single crystals of the HYIG  $\text{HO}_x\text{Y}_{3-x}\text{Fe}_5\text{O}_{12}$  were grown by spontaneous crystallization from the solution in the melt (see Ref. 8 for more details). The composition of the samples was determined by x-ray spectral analysis, and also by measurements of the saturation magnetization in the  $\langle 111 \rangle$  direction at 4.2 K (as shown in Ref. 8, the magnetization of HYIG per mole depends linearly on the holmium concentration).

The magnetization was measured in static fields up to 70 kOe with a vibration magnetometer, and also in pulsed fields up to 300 kOe by an induction method. The critical fields of the phase transitions were determined, in addition, from measurements of the differential susceptibility in pulsed fields. The torque acting on the single crystal was measured in pulsed fields up to 120 kOe using a setup with a piezoelectric pickup (in our version the pickup used was single-crystal quartz), similar to the setup described earlier.<sup>9</sup> All the measurements were made at 4.2 K.

#### 5. EXPERIMENTAL DATA AND THEIR THEORETICAL INTERPRETATION

Figure 2a shows the experimental dependences of the magnetization on the field in HYIG  $\text{HO}_{0.41}\text{Y}_{2.59}\text{Fe}_5\text{O}_{12}$  along the crystallographic directions  $\langle 100 \rangle$ ,  $\langle 110 \rangle$ ,  $\langle 111 \rangle$ . It is seen that in fields of the order of 100 kOe the plots of the magnetization against the field show jumps, one in a field parallel to the  $\langle 100 \rangle$  axis and two in a field parallel to the  $\langle 110 \rangle$  axis, and three in a field

parallel to the  $\langle 111 \rangle$  axes. The jumps exhibit hysteresis: when the field is increased the jumps occur in stronger fields than in a decreasing field. We note that in a field parallel to the  $\langle 111 \rangle$  axis, which is an easy-magnetization axis, absolute saturation is reached after the jumps—the magnetization becomes equal to the sum of the magnetic moments of the iron and rare-earth sublattices.

The magnetization behaves anomalously also in weaker fields (see the inset of Fig. 2a). Whereas the magnetization along the  $\langle 111 \rangle$  axes saturates in weaker fields and depends little on the field if it is weaker than the jump field, the magnetization along the  $\langle 110 \rangle$  and  $\langle 100 \rangle$  axes increases with the field, and in a certain value of the field the magnetization in these directions becomes larger than the magnetization in the easy direction  $\langle 111 \rangle$ .

Similar magnetization curves are observed for other compositions of HYIG with  $x < 0.8$  ( $x = 0.8$  is the concentration at which the magnetic moment of the rare-earth sublattice, i.e.,  $m_R = 1$ , and the total magnetization of the HYIG with  $x = 0.8$  is equal to zero). The increase of  $x$  in this concentration range, without changing the number of jumps along different directions, leads only to a change in the transition fields, a change in the amplitude of the jumps, and also to an increase of the hysteresis in the transitions.

Different dependences of the magnetization on the field are observed in HYIG with large holmium contents. Figure 3a shows the magnetization curves of  $\text{HO}_{1.05}\text{Y}_{1.95}\text{Fe}_5\text{O}_{12}$ . It is seen that the magnetization curve has in a field parallel to the  $\langle 111 \rangle$  axis two anomalies, past which the magnetization reaches absolute saturation. When the field is oriented along  $\langle 110 \rangle$  and  $\langle 100 \rangle$  an increase of the magnetization is observed with increasing field, but there are no jumps. Nonetheless, even for this HYIG the magnetization in the easy direction  $\langle 111 \rangle$  becomes smaller in a certain field interval than in the directions  $\langle 110 \rangle$  and  $\langle 100 \rangle$ . Similar dependences of the magnetization on the field are observed for other HYIG samples in the concentration  $0.8 < x \leq 1.25$ .

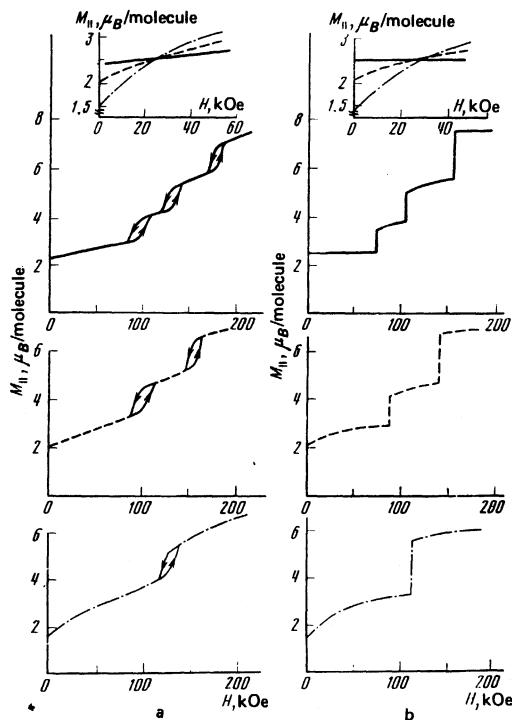


FIG. 2. Experimental (a) and theoretical (b) plots of the magnetization of the HYIG  $\text{HO}_{0.41}\text{Y}_{2.59}\text{Fe}_5\text{O}_{12}$  against the field: solid curves—for  $H \parallel \langle 111 \rangle$ , dashed—for  $H \parallel \langle 110 \rangle$ , dash-dot—for  $H \parallel \langle 100 \rangle$ . The insets show  $M_{\parallel}(H)$  in weak fields.

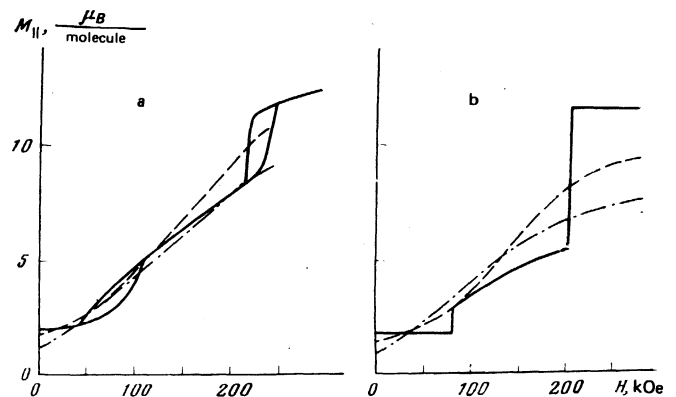


FIG. 3. Experimental (a) and theoretical (b) plots of the magnetization of the HYIG  $\text{HO}_{1.05}\text{Y}_{1.95}\text{Fe}_5\text{O}_{12}$  against the field: solid lines—for  $H \parallel \langle 111 \rangle$ , dashed—for  $H \parallel \langle 110 \rangle$ , dash-dot—for  $H \parallel \langle 100 \rangle$ .

Our measurements have shown that the magnetization of the single-crystal HYIG  $\text{HO}_{1.65}\text{Y}_{1.35}\text{Fe}_5\text{O}_{12}$  along the  $\langle 111 \rangle$  axis begins to increase when a field  $H_1 = 200$  kOe is reached. This increase takes place (in contrast to samples with smaller holmium contents) without hysteresis, smoothly, and absolute saturation is not reached in fields accessible to us. Linear extrapolation of the experimental data yields for the saturation field  $H_2 = 320$  kOe. For this sample, the magnetization in the directions  $\langle 100 \rangle$ ,  $\langle 110 \rangle$  also exceeds in a certain field interval the magnetization in the easy direction  $\langle 111 \rangle$ .

In HYIG with  $x > 1.65$  (2.5; 3) we observe no anomalies of the magnetization. They apparently lie in fields stronger than experimentally obtained in our study ( $\sim 300$  kOe).

Most of our experimental results can be well explained within the framework of the theory developed above for the magnetization of iron garnets with Ising rare-earth ions.

The anomalies of the magnetization of HYIG are due to a  $180^\circ$  reorientation, in the field, of the magnetic moments of the  $\text{HO}^{3+}$  ions in different nonequivalent positions (this, as indicated, is equivalent to reorientation of the resultant moment of the holmium sublattice from one direction of the  $\langle 111 \rangle$  type to another) and to the corresponding rotation of the magnetic moment of the iron sublattice, and the theory predicts correctly the number of anomalies of the magnetization along different directions and its change with increasing holmium concentration in the HYIG: at  $x < 0.8$  one observes in experiment three jumps in a field parallel to a  $\langle 111 \rangle$  axis, two in a field parallel to  $\langle 110 \rangle$ , and one in a field parallel to  $\langle 100 \rangle$ ; at larger contents of holmium, the anomalies of the magnetization take place when the field is oriented in an  $\langle 111 \rangle$  direction—two at  $0.8 < x \leq 1.25$  and one at  $x = 1.65$ .

Moreover, the theory yields phase-transition fields that agree with experiment and describe satisfactorily the experimentally obtained dependences of the magnetization on the field for HYIG with  $x < 1.65$ . This is clearly seen from the theoretical magnetization curves of the corresponding HYIG shown in Figs. 2b and 3b. However, for the  $\text{HO}_{1.65}\text{Y}_{1.35}\text{Fe}_5\text{O}_{12}$  sample the theory does not yield the experimentally observed smooth increase of the magnetization along the  $\langle 111 \rangle$  axis. The causes will be discussed below. We note that no fit parameters whatever were used in the theoretical calculation, and the values of the molecular field  $H_{\text{mol}} = \lambda_{\text{Fe}}$  and of the magnetic moment of the holmium ion  $\mu_{\text{HO}}$ , which are needed for the calculation, were taken from the results of independent measurements on holmium iron garnet:  $H_{\text{mol}} = 125$  kOe from Ref. 10<sup>3)</sup> and  $\mu_{\text{HO}} = 11\mu_{\text{B}}$  from Ref. 8 (in the calculation of  $\mu_{\text{HO}}$  from the experimental data it was assumed that the holmium ions have an Ising magnetic ordering).

From the theory developed above follow also the experimentally observable intersections of the magnetization curves along different directions (see the insets of

Fig. 2, and also Fig. 3). These intersections are physically due to the fact that, as already noted, at  $H \parallel \langle 111 \rangle$  in fields weaker than the field of the first phase transition the magnetic moments of the iron and resultant holmium sublattices remain antiparallel (collinear phase), and according to the theoretical model the magnetization must not vary with the field in this field interval. On the other hand, if the field is oriented at an angle to the easy-magnetization axis, then even in weak fields a noncollinear structure is produced, in which the magnetic moment of the iron sublattice deviates from the  $\langle 111 \rangle$  axis towards the field direction, and the moment of the resultant holmium sublattice remains oriented along this axis, owing to the Ising character of the magnetic ordering. Because of this, the magnetization increases with increasing field, and exceeds in a certain field the magnetization along the  $\langle 111 \rangle$  axis.

Figure 4 shows the experimental  $H$ - $x$  phase diagrams of the HYIG  $\text{Ho}_x\text{Y}_{3-x}\text{Fe}_5\text{O}_{12}$  for field orientations along the axes  $\langle 100 \rangle$ ,  $\langle 110 \rangle$ ,  $\langle 111 \rangle$ . The same figure shows the theoretical phase diagrams for IG with Ising rare-earth ions, constructed in accordance with formulas (14)–(20) and using the cited values of  $H_{\text{mol}}$  and  $\mu_{\text{HO}}$ . It is seen that the experimental and theoretical plots of the critical fields against the holmium concentration are in agreement. We note that the theoretical values of the critical fields correspond, as indicated above, to equality of the energies of the different phases. Experiment, on the other hand, reveals hysteresis of the transition fields (Fig. 4 shows the critical fields with

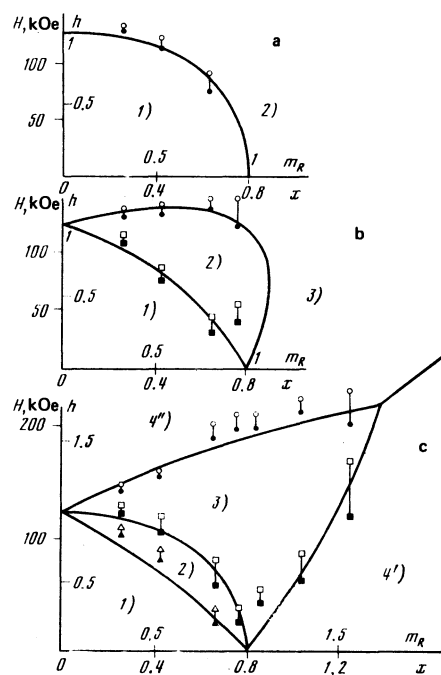


FIG. 4.  $H$ - $x$  phase diagrams of the HYIG  $\text{Ho}_x\text{Y}_{3-x}\text{Fe}_5\text{O}_{12}$  along the crystallographic axes  $\langle 100 \rangle$  (a),  $\langle 110 \rangle$  (b), and  $\langle 111 \rangle$  (c). Circles, squares, and triangles—experimental values of the jump fields (light symbols—with increasing field, dark—with decreasing field). Solid lines—theoretical calculations. The numbers denote the phases.

increasing and decreasing field). This hysteresis can be due to the existence of metastable states, or apparently also to relaxation processes (the transition hysteresis is weaker in static than in pulsed fields). However, the experimental value of the hysteresis is much less than would follow from theoretical estimates of the region of metastability of the different phases. Thus, metastable states are not fully realized in such transitions. It is possible, however, that the onset of metastability causes the transitions to become smeared out in a number of cases over a finite field interval (other probable causes of this phenomenon will be considered below).

In the discussion of the theoretical model it was noted that if the field is oriented in an arbitrary direction in a plane of the  $\{110\}$  type, the largest possible number of transitions is equal to five. Experiment confirms this conclusion. Figure 5a shows the experiment  $H-\varphi$  phase diagram of the HYIG  $\text{HO}_{0.41}\text{Y}_{3.59}\text{Fe}_5\text{O}_{12}$  in the  $\{110\}$  plane. It is seen that at certain orientations of the field there are five phase transitions, and the experimental dependence of the transition fields on the angle agrees qualitatively with the theoretical one (Fig. 5b), although there are some quantitative differences between them.

Interesting data on the processes of HYIG magnetization can be obtained from the plots of the torque against the field. Figure 6a shows an experimental plot of  $L(H)$  in the  $\{110\}$  plane of the HYIG  $\text{HO}_{0.41}\text{Y}_{2.59}\text{Fe}_5\text{O}_{12}$ . It is seen that the torque has an unusual behavior: with increasing field the sign of  $L$  is reversed. This behavior agrees qualitatively with the Ising model of magnetic ordering of this ferrimagnet. As follows from the thermodynamic relations, in the most general form the torque, in relative units, can be represented in the form

$$L = m_{\perp} h, \quad (22)$$

where  $m_{\perp}$  is the projection of the relative magnetization of the HYIG on the direction perpendicular to the field and to the rotation axis. It is seen from (10) that  $m_{\perp}$  consists of two terms: the projection  $\gamma_1$  of the iron sublattice and the projection  $m_{R_1}$  of the resultant rare-earth sublattice. In a zero field,  $\gamma$  is antiparallel to

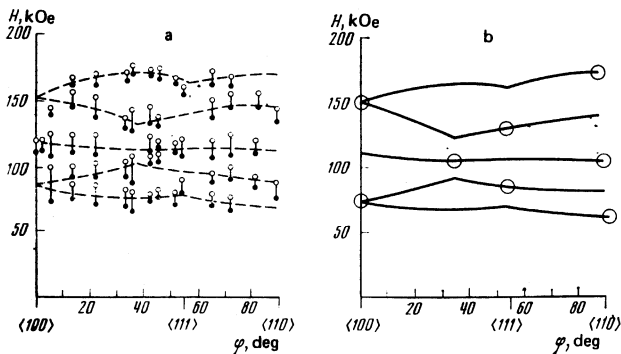


FIG. 5. Experimental (a) and theoretical (b)  $H-\varphi$  phase diagram of the HYIG  $\text{HO}_{0.41}\text{Y}_{2.59}\text{Fe}_5\text{O}_{12}$  in the  $\{110\}$  plane. The circles show the angles at which the values of the corresponding jumps are equal to zero.

$m_R$ , so that for this HYIG we have  $m_R < 1$  and the resultant torque is determined by the iron sublattice. With increasing field, the magnetic moment of the iron sublattice begins to rotate towards the field direction,  $\gamma_1$  decreases, whereas the magnetic moment of the rare-earth sublattice does not change its direction because of the Ising character of the ordering of the rare-earth ions. Consequently,  $m_{R_1}$  like-wise remains unchanged. Therefore in a certain field  $m_{R_1}$  becomes larger than  $\gamma_1$ , and this leads to a change in the sign of the torque.

The torque changes sign also in the phase-transition field. Using (10), we easily obtain a general expression for the torque of the HYIG at a field orientation in the (111) plane for the  $i$ -th phase ( $i = 1-6$ ) (see Sec. 3):

$$L = h(1 - |h - m_R^{(i)}|^{-1}) [2^{-1/2} \cos \varphi (m_{Rx}^{(i)} + m_{Ry}^{(i)}) - m_{Rz}^{(i)} \sin \varphi], \quad (23)$$

where the angle  $\varphi$ , which determines the orientation of the external field, is measured from the  $[001]$  axis, and  $m_{R\alpha}^{(i)}$  ( $\alpha = x, y, z$  are the components of the vectors  $m_R^{(i)}$  in the crystallographic axes. The torque curve calculated from this formula for a HYIG with  $x = 0.41$  is shown in Fig. 6b and agrees well with the experimental relation, as follows from a comparison with Fig. 6a.

## CONCLUSION

The reported experimental results and their comparison with the theoretical calculations show that many properties of HYIG can be described in a model wherein the magnetic ordering of the  $\text{HO}^{3+}$  ions in the garnet structure is of the Ising type. The form of the magnetization curves in weak fields, the number and magnitude of the anomalies of the magnetizations of different compositions when the field is oriented along different directions, the  $H-x$  and  $H-\varphi$  phase diagrams, the field dependences of the torque, are all described by this model, as already noted, without resorting to any additional fit parameters whatever.

There are, however, a number of facts that cannot be described in this simple model.

1. The pure Ising model is in poor agreement with neutron-diffraction data,<sup>13,14</sup> according to which the magnetic moments of the holmium in  $\text{HO}_3\text{Fe}_5\text{O}_{12}$  form a double "umbrella" with inclination angles from the  $\langle 111 \rangle$  axis in the planes  $\{110\}$  amounting to 29 and 63°, and not to 55° as should be the case of the Ising model.<sup>4)</sup>

2. Whereas in the Ising model of the ordering of the

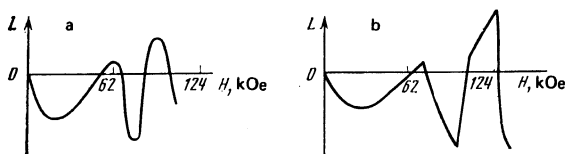


FIG. 6. Experimental (a) and theoretical (b) plots of the torque of the HYIG  $\text{HO}_{0.41}\text{Y}_{2.59}\text{Fe}_5\text{O}_{12}$  in the  $\{110\}$  plane. The field is oriented at an angle 80° to the  $\langle 100 \rangle$  axis.

rare-earth ions the magnetization along the  $\langle 111 \rangle$  axis should not depend on the field in weak fields, for in this case the "umbrella" should not be deformed, the experimental  $M \parallel (H)$  curves along this direction reveal an increase of the magnetization with increasing field, which is particularly noticeable in compositions with large holmium content, for example in holmium iron garnet.<sup>15,16</sup>

3. In the Ising model transitions from one phase to another should proceed jumpwise. The anomalies on the experimental plots of the magnetization against the field in HYIG stretch in a number of cases over a certain field interval, this being particularly noticeable for composition with large holmium contents. As already noted, this can be due to the onset of metastable states. but this smearing is largest for the transition 4')  $\approx$  4") in HYIG with  $x = 1.65$ , where there is not metastability under the model under consideration.<sup>5)</sup>

All these singularities can be qualitatively explained by assuming that the Ising model is a first approximation, and that the holmium ion in the HYIG, while strongly anisotropic, is not a pure Ising ion. In other words, differing from zero are not only the  $z_i$  components, but also other magnetic-moment components of the holmium ion, and consequently deviations (albeit small ones) of the magnetic moment of the corresponding holmium sublattice from an axis of the  $\langle 100 \rangle$  type are possible. The crystal field in the exchange interaction between the holmium and iron ions lead to the existence of an umbrella arrangement of the magnetic moments of the holmium ions, with angles different from  $55^\circ$ , and the external field leads to a change of this angle. This assumption provides also a natural explanation for the fact that the Ising model becomes less effective when the holmium concentration is increased, and why, for example, the 4')  $\approx$  4") in HYIG with  $x = 1.65$  proceeds smoothly at  $H \parallel \langle 111 \rangle$  and becomes similar to the transition in the isotropic model. In the 4')  $\approx$  4") transition, as already noted, the magnetic moment of the iron sublattices is rotated through  $180^\circ$ . If the rare-earth ions are of the Ising type, so that the resultant magnetic moment of the rare-earth sublattice cannot deviate from the  $\langle 111 \rangle$  axis, then this transition must take place jumpwise. On the other hand, if such deviations are possible, then the reorientation of the magnetic moment of the iron sublattice takes place gradually and is accompanied by a deviation of the magnetic moment of the resultant rare-earth sublattice from this axis.

By using, for example, the relations given in Ref. 1, it is easy to find that in the isotropic approximation the maximum deviation angle of the magnetic moment of the rare-earth sublattice is

$$(\theta_n)_{\max} = \arccos[(1 - m_n^{-2})^{1/2}], \quad (24)$$

i.e., the larger  $m_R$ , the smaller the deviation of the magnetic moment of the rare-earth sublattice from the  $\langle 111 \rangle$  axis, and therefore at large holmium contents even a small deviation of the components  $m_{R_x}$  and  $m_{R_y}$  from zero causes the transition in question to become smooth. Estimates show that for HYIG with  $x = 1.65$  it suffices for this purpose to have  $m_{R_x} m_{R_y} < 0.1 m_{R_z}$ .

From the microscopic point of view, the deviations from the Ising model can be qualitatively explained by recognizing that our analysis was restricted to consideration of the ground quasidoublet of the  $HO^{3+}$  ion in a crystal field, and it is this which caused the pure Ising character of the behavior of the magnetic moments of the  $HO^{3+}$  ions, and we neglected the influence of the higher levels. Allowance for the influence of the higher levels (by perturbation theory) adds to the energy of the ground state of the  $HO^{3+}$  ion in the  $i$ -th site the increments

$$\Delta E_i = - \sum_{\alpha=x,y,z} \delta_\alpha [(H - \lambda M_{Fe}) \alpha_i]^2 + \dots, \quad (25)$$

where  $\alpha_i$  is the orientation of the symmetry axes of the  $i$ -th site,  $\delta_\alpha > 0$  are numerical coefficients that depend on the spectrum and on the wave functions of the ion in the crystal field. It is these increments which make the  $HO^{3+}$  ions no longer of pure Ising type, and makes it possible for their magnetic moments to deviate from axes of the  $\langle 100 \rangle$  type.

From this point of view, the increase of the deviation from the Ising model in compositions with large holmium contents can be attributed to the behavior of the energy levels of the  $HO^{3+}$  ion in a magnetic field. As noted above, the Ising approximation holds true in the case when the ground quasidoublet is separated from the ground levels by a large distance and the interaction of the levels of a quasidoublet with the higher levels can be neglected. In compositions with small holmium contents ( $m_R < 1$ ) the external field is oriented antiparallel to the exchange fields, and therefore leads to a decrease in the splitting of the levels of the quasidoublet and to an increase of the distance from the excited level of a quasidoublet to the higher levels. In other words, in this case the external field can only contribute to an Ising character of the spins. On the other hand if the holmium content is high ( $m_R > 1$ ), then the external field is parallel to the exchange field and leads to an increase of the splitting of the quasidoublet levels, to an approach of one of the doublet components to the higher levels, i.e., the Ising character of the spins is violated.

We note that the Kramers ion  $Dy^{3+}$  in the aluminate garnet  $Dy_3Al_5O_{12}$  is almost of the Ising type.<sup>17</sup> The splitting of its ground doublet by the exchange and external fields is of the form

$$E_{1,2} = \pm (g_x^2 H_{\text{eff } x}^2 + g_y^2 H_{\text{eff } y}^2 + g_z^2 H_{\text{eff } z}^2)^{1/2},$$

where  $g_x, g_y \ll g_z$  (for  $Dy_3Al_5O_{12}$  we have<sup>17</sup>  $g_x = 0.73, g_y = 0.40, g_z = 18.2$ ).

A similar situation can arise for a non-Kramers  $HO^{3+}$  ion in an iron garnet, if its ground state in the crystal field is a quasitriplet. It is easy to show that in the general case the splitting of the quasitriplet can be represented in the form

$$E_{1,2} = \pm (\mu_x^2 H_{\text{eff } x}^2 + \mu_y^2 H_{\text{eff } y}^2 + \mu_z^2 H_{\text{eff } z}^2)^{1/2}, \quad E_3 = 0.$$

If  $\mu_x = \mu_y = 0$ , then we are dealing with the pure Ising model considered above. A deviation from Ising behavior takes place as a result of the deviation of  $\mu_x$

and  $\mu_y$  from zero.

The authors thank K. P. Belov for interest in the work and for valuable remarks, and A. S. Markosyan and B. V. Mill' for growing the iron-garnet single crystals.

- <sup>1</sup>In this model we neglect the magnetic anisotropy of the iron sublattice because it is small compared with the magnetic anisotropy of the rare-earth ions.
- <sup>2</sup>In order not to encumber the exposition with a large number of formulas we do not list here and below the regions where the phases exist. We note only that with increasing concentration of the rare-earth ions the hysteresis near the phase-transition lines increases.
- <sup>3</sup>We note that in the literature there are also other values of  $H_{mo1}$  for holmium iron garnet, ranging from 109 (ref. 11) to 147 kOe (ref. 12). The use of these values in the calculation leads only to changes in the fields of the phase transitions, without changing the general form of the magnetization curves and of the phase diagrams. The best agreement between theory and experiment is obtained at  $H_{mo1} = 125$  kOe.
- <sup>4</sup>Incidentally, it should be noted that neutron-diffraction data were obtained under a number of assumptions. In some cases (for example for  $Er_3Fe_5O_{12}$ ) they contradict the results of later magnetic measurements.<sup>15</sup>
- <sup>5</sup>Allowance for the magnetic anisotropy of the iron sublattice does not lead to agreement with experiment.
- <sup>1</sup>K. P. Belov, *Ferrity v sil'nykh polyakh (Ferrites in Strong Fields)*, Nauka, 1975.
- <sup>2</sup>S. V. Tyablikov, *Metody kvantovoi teorii magnetizma (Methods of the Quantum Theory of Magnetism)*, Nauka, 1965.
- A. Clark and E. Callen, *J. Appl. Phys.* **39**, 5972 (1968).

- <sup>3</sup>A. K. Zvezdin, *Pis'ma Zh. Eksp. Teor. Fiz.* **10**, 196 (1969) [*JETP Lett.* **10**, 124 (1972)]. A. K. Zvezdin and V. M. Matveev, *Zh. Eksp. Teor. Fiz.* **62**, 260 (1972) [*Sov. Phys. JETP* **35**, 140 (1972)]. N. F. Kharchenko, V. V. Eremenko, S. L. Gnatchenko, L. I. Belyi, and E. M. Kabanova, *Zh. Eksp. Teor. Fiz.* **68**, 1073 (1975) [*Sov. Phys. JETP* **41**, 531 (1975)].
- <sup>4</sup>V. G. Demidov and R. Z. Levitin, *Zh. Eksp. Teor. Fiz.* **72**, 1111 (1977) [*Sov. Phys. JETP* **45**, 581 (1977)].
- <sup>5</sup>A. K. Zvezdin, A. A. Mukhin, and A. I. Popov, *Zh. Eksp. Teor. Fiz.* **72**, 1097 (1977) [*Sov. Phys. JETP* **45**, 573 (1977)].
- <sup>6</sup>D. Boal, P. Grunberg, and J. Koningsstein, *Phys. Rev. B* **7**, 4757 (1973). V. Nekvasil, *Phys. Status Solidi B* **94**, K41 (1979).
- <sup>7</sup>J. Griffith, *Phys. Rev.* **132**, 316 (1963).
- <sup>8</sup>A. K. Gapeev, R. Z. Levitin, A. S. Markosyan, E. V. Mill', and T. M. Perekalina, *Zh. Eksp. Teor. Fiz.* **67**, 232 (1974) [*Sov. Phys. JETP* **40**, 117 (1975)].
- <sup>9</sup>B. K. Ponomarev and R. Z. Levitin, *Prib. Tekh. Éksp.* No. 3, 188 (1966).
- <sup>10</sup>M. Guilot, P. Feldmann, H. Le Gall, and M. Fadly, *IEEE Trans. Magn. (MAG-14)*, 909 (1978).
- <sup>11</sup>R. Z. Levitin, B. K. Ponomarev, and Yu. F. Popov, *Zh. Eksp. Teor. Fiz.* **59**, 1952 (1970) [*Sov. Phys. JETP* **32**, 1056 (1970)].
- <sup>12</sup>M. Balanda and S. Niziol, *Phys. Status Solidi B* **91**, 291 (1979).
- <sup>13</sup>V. Allain, M. Bihara, and A. Herpin, *J. Appl. Phys.* **37**, 1316 (1966).
- <sup>14</sup>A. Herpin, W. Kochler, and P. Meriel, *C. R. Acad. Sci.* **251**, 1359 (1960).
- <sup>15</sup>V. G. Demidov, Abstract of Candidate's dissertation, Moscow State Univ., 1977.
- <sup>16</sup>A. Herpin, *Theorie du magnetisme*, 1977.
- <sup>17</sup>K. P. Belov and V. I. Sokolov, *Usp. Fiz. Nauk* **121**, 285 (1977) [*Sov. Phys. Usp.* **20**, 149 (1977)].

Translated by J. G. Adashko